

Article

Evaluation of Heat Transfer Performance of a Multi-Disc Sorption Bed Dedicated for Adsorption Cooling Technology

Marcin Sosnowski 

Faculty of Science and Technology, Jan Dlugosz University in Czestochowa, Czestochowa, Armii Krajowej 13/15 42-200, Poland; m.sosnowski@ujd.edu.pl; Tel.: +48-34-36-12179

Received: 10 November 2019; Accepted: 6 December 2019; Published: 8 December 2019



Abstract: The possibility of implementing the innovative multi-disc sorption bed combined with the heat exchanger into the adsorption cooling technology is investigated experimentally and numerically in the paper. The developed in-house sorption model incorporated into the commercial computational fluid dynamics (CFD) code was applied within the analysis. The research allowed to define the design parameters of the proposed type of the sorption bed and correlate them with basic factors influencing the performance of the sorption bed and its dimensions. The designed multi-disc sorption bed is characterized by great scalability and allows to significantly expand the potential installation sites of the adsorption chillers.

Keywords: adsorption; cooling technology; chiller; heat exchanger; waste heat utilization; CFD

1. Adsorption Cooling Technology

1.1. Environmental Demands

Energy and environment-related issues are strongly inter-related and are becoming the most important and popular topics in research activities nowadays [1]. The European Union's concerns are focused on energetic efficiency as the most effective method of reducing primary energy consumption. It directly lowers the emissions of harmful substances into the atmosphere and, consequently, improves air quality. An important element of activities aimed at increasing energetic efficiency is the maximum use of heat that has so far been released into the atmosphere and its conversion into usable energy. Moreover, the two main expectations defined in the concept of sustainable development are the reduction of energy consumption from non-renewable sources and the effective utilization of low-grade thermal energy originating from industrial waste heat, solar power, cogeneration or exhaust gases from internal combustion engines [2].

On the other hand, the demand for cooling in the industrial and residential sectors is increasing. The mechanical vapor-compression air-conditioning systems are commonly used to meet such a demand for cooling and their popularity results from high coefficients of performance (COP), small sizes, and low weights. Unfortunately, they vastly contribute to the global warming and ozone layer depletion because of the usage of refrigerants such as chlorofluorocarbon, hydro-chlorofluorocarbon, or hydrofluorocarbons [3]. Therefore, the development and wide-spread usage of an alternative solution to the conventional cooling systems is a necessity.

1.2. Adsorption Chillers

The devices, which are capable to generate chill on the ground of adsorption cooling technology can be the perfect solution to the aforementioned issues [4–6]. The adsorption chillers can be

successfully powered with low-grade heat, which can be obtained from renewable sources, e.g., solar radiation [6], geothermal energy [7], or industrial waste heat [8–11]. They can be applied in combined cooling, heating, and power (CCHP) systems in numerous industrial and commercial applications [12] as well as in sustainable building air-conditioning using solar energy as heat source [1]. The production of chill, practically without the use of electricity, by absorption chillers, has a particular significance in summer, during the peak period of demand for electricity from the network to supply conventional vapor-compression refrigeration systems. In addition, the adsorbents in the adsorption cooling technology are porous materials like silica gel, zeolites, and activated carbons, which are environmentally friendly with no impact to the atmosphere [13]. The adsorbates are natural coolants such as water, ethanol, methanol, CO₂, or ammonia. These working pairs in adsorption cooling technology are characterized by zero global warming potential (GPW) and ozone depletion potential (ODP) [14].

Other important benefits of adsorption chillers in comparison to conventional vapor-compression systems are driving these devices with renewable or waste heat source of temperature as low as 50 °C [7], which directly leads to a reduction in CO₂ emissions and pollution [15], almost zero electricity consumption [6], no moving parts resulting in high reliability [16], simple control and maintenance [3]. Moreover, on the markets of the Middle and the Far East, adsorption technology is intensively developed because of the possibility of desalination of seawater along with the production of cooling energy [17]. But the widespread application of adsorption chillers is limited by the following shortcomings of adsorption cooling technology: low coefficient of performance [18], large weight and volume [16], intermittent cooling [14], high initial procurement cost [14], and exploitation under vacuum conditions [2].

1.3. Design and Operation

The adsorption phenomenon is the binding of the adsorbate to the surface of the adsorbent. The adsorption cooling technology utilizes the physical sorption phenomenon, where the molecules of adsorbate are bound to the surface of the porous adsorbent by Van-der-Waals forces [16]. These are intermolecular interactions between two dipoles, one of which is induced by another permanent dipole [15]. The combination of subsequent adsorption and desorption cycles is used to produce the cooling effect in the adsorption cooling technology.

The single-bed, single-stage adsorption chiller consists of an evaporator, condenser, valves separating adjacent devices, and at least one sorption bed [19] as shown in Figure 1a. The advances in the design of evaporators and condensers are described in [20,21]. The sorption bed is designed as a hermetic container with a built-in heat exchanger, which transfers heat between the sorbent and the heating/cooling medium (usually water). More than one sorption bed can be applied in order to reduce the intermittency of chill production and assure heat and mass recuperation. The granular packed adsorbent bed design is usually used in the adsorption cooling systems [12] because it is characterized by high mass transfer performance due to the high permeability level and developed specific surface of the adsorbents.

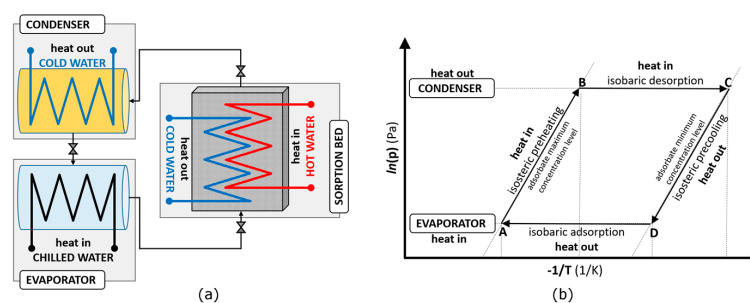


Figure 1. Basic, single-bed, single-stage adsorption cooling system: (a) chiller design; (b) Clapeyron diagram.

The ideal adsorption refrigeration cycle is typically expressed by the Clapeyron diagram [22] with respect to the isosteres of adsorbent–adsorbate pair as shown in Figure 1b. The sorption bed operates between the condenser pressure and the evaporator pressure as well as the minimum and maximum adsorbate concentration levels. The Clapeyron diagram (Figure 1b) illustrates the four ideal thermodynamic steps occurring in the bed i.e., isosteric preheating (A–B), isobaric desorption (B–C), isosteric precooling (C–D), and isobaric adsorption (D–A) [23].

The absorptivity of the adsorbent is directly proportional to the pressure. The adsorption conducted under high pressure would be optimal because of the use of the absorptive capacity of the bed; however, the adsorbate vapor temperature is strictly correlated with the pressure. In the evaporator, intensively evaporating adsorbate under reduced pressure rejects heat from the chilled water, thus generating the cooling power. That is why the chilled water temperature is related to the evaporator pressure; the lowest chilled water temperatures are achievable at low adsorption pressures. It is, therefore, necessary to balance between a low temperature of the obtained chill and the efficiency of the device.

1.4. Literature Review

The literature reports valuable examples of research concerning the adsorption cooling technology. Sakoda and Suzuki performed a fundamental study on solar-powered, silica gel–water adsorption cooling system [24]. They also analyzed the transport of heat and adsorbate in a small-scale unit on the ground of both experimental and numerical research [25]. Numerous research report the potential for applying different heat transfer enhancements techniques to improve adsorption bed thermal performance. One of them is based on replacing the gaseous voids of low thermal conductivity between the individual grains of sorbent with the glue of better thermal properties as was investigated in [26–31]. The obtained results confirmed the beneficial influence of this technique on the COP. Aristov et al. [32] optimized the adsorption dynamics with the application of loose-grain sorbent. The insertion of metallic additives to the sorbent was investigated in [12,33]. Another approach based on a polydispersed composition of the sorption bed was analyzed by Girnîk and Aristov [34] and Demir et al. [35]. Alam et al. [36] numerically investigated the heat exchanger design effect on the performance of closed cycle, two-bed adsorption cooling systems. The authors defined a non-dimensional switching frequency and studied the effect of heat exchanger design parameters on the system performance. The modifications of the heat exchanger design were also investigated in [18,37,38]. Ilis et al. [39] performed very interesting research concerning the innovative star fin type adsorbent bed design. Two dimensional numerical analysis allowed to determine the optimum geometrical parameters and find the best specific cooling performance value. Moreover, the influence of metal additives on the performance of the adsorption chiller was investigated. The finned tube heat exchanger was analyzed in [40] and flat-tube heat exchanger was examined in [41]. A 2D coupled heat and mass transfer model was used in [42] to analyze the performance of both finless and finned tube-type adsorbent beds during only the desorption mode. A significant enhancement in the heat transfer was obtained using a finned tube adsorbent bed. The effect of fin design parameters on the heat transfer inside the bed was also investigated using four different fin configurations.

Researches evaluated different adsorption pairs [43,44] but silica gel/water has shown significant advantages in terms of thermal performance and environmental impact [12]. Water vapor as adsorbate is characterized by excellent thermo-physical properties of high latent heat of evaporation, high thermal conductivity, low viscosity, and thermal stability in a wide range of operating temperatures. Silica gel is a synthetically obtained porous form of silicon oxide (SiO_2) characterized by high chemical resistance. The advantages of silica gel as adsorbent are also revealed in high adsorption/desorption rate, low regeneration heat, good long-term stability, and minimal hysteresis [45]. The analysis of the thermal behavior of devices using silica gel shows that their performance is very sensitive to heat and mass transfer rates inside the adsorbent beds [46]. According to [47], the lowest temperature needed to regenerate the adsorption chiller bed is required for the silica gel–water pair. Therefore, this sorption

pair opens up a number of chiller's possible applications because of the low temperature of the required heat source.

Apart from experimental research, several numerical methods were applied in studies on adsorption cooling technology. Krzywanski et al. [48–50] successfully utilized the genetic algorithms, neural networks, and AI approach for adsorption chiller work cycle analysis. The rapid development of high-performance computing (HPC) resulted in the increasing scope of computational fluid dynamics (CFD) application, also in the area of adsorption technology. Papakokkinos et al. [51] presented a generalized three-dimensional CFD model based on the unstructured meshes. Dynamic conjugate simulations of the packed bed and the heat exchanger allowed to study the influence of sorption bed geometry on the reactor performance. The effect of the adsorbed mass spatial distribution on the desorption phase was also discussed and the strong impact of the solid volume fraction, fin length, and fin thickness on the heat transfer was demonstrated. A similar parametric study concerning finned tube heat exchanger was performed in [37]. Detailed analysis of flow characteristics and heat transfer within a packed bed of sorbent using CFD technique were also performed in [52–55]. This research tool was also applied in studies dealing in adsorption dynamics of cylindrical silica gel particles [56], where authors adopted a three-dimensional finite volume method for solving the coupled energy and mass diffusion equations.

1.5. The Main Aim of the Work

The key challenges in the development of the adsorption cooling technology are the low performance and large dimensions of the adsorption chillers. Enhancing the adsorption kinetics by improving heat and mass transfer is necessary in order to improve the adsorption chiller performance [12]. Both, performance and dimensions of the device are dependent on the design of a heat exchanger constituting the adsorption bed [57,58], which is the most important part of the chiller [14]. That is why the advances in the heat exchanger design will directly contribute to diminishing the drawbacks of these environmentally friendly devices.

Therefore, the aim of this research is to investigate the possibility of implementing the innovative multi-disc sorption bed in an adsorption cooling technology in order to increase the COP of adsorption cooling devices by intensifying the heat transfer in a sorption bed as well as open up the possibilities of wider use of adsorption chillers because of the scalable and flat design of the bed.

2. Research Object

2.1. Multi-Disc Sorption Bed Design

The innovative construction of a multi-disc sorption bed proposed by the author and depicted in Figure 2 is investigated in this research. In contrast to the commonly-applied designs, in a multi-disc bed, the sorbent is placed in many separate disc-shaped packets, and the cooling/heating water washes the packets of sorbet from the outside transferring heat. The adsorbate vapor flows through the fixing net into the sorbent packets penetrating them. The fixing net holds the granular sorbent inside the disc-shaped packets.

The proposed construction allows to place the device e.g., in the ceiling of the building or integrate it with solar panels, which will supply the device with the necessary heat. Such a solution allows to significantly expand the potential installation sites of the adsorption chillers and thus reduce one of the main disadvantages of these devices, which is the need to save a large space for the installation of the adsorption chiller. Another advantage of the proposed solution is its potential for scalability consisting of adjusting the number of sorbent discs to the expected cooling capacity of the device or the possibility of installing two or more multi-disc sorption beds with sorbent packages one above another with the space between them being a vapor collector.

The analysis of the commercially available adsorption cooling equipment and the literature review showed that the presented solution is not the current state of the research field. Therefore, a patent

application was prepared for the Polish Patent Office on the basis of the presented multi-disc sorption bed design.

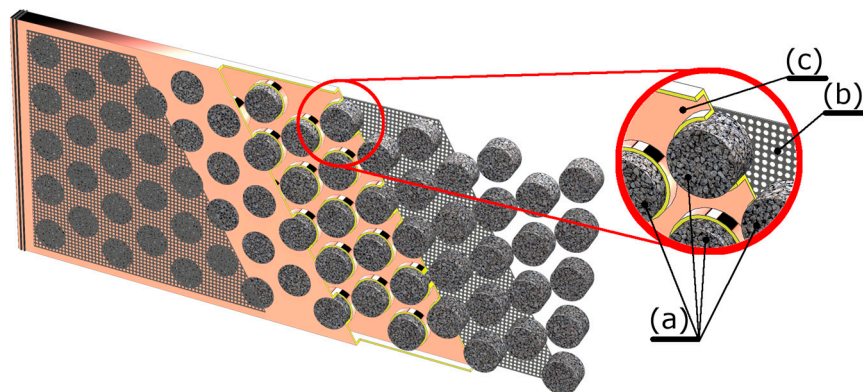


Figure 2. Sectional view of the investigated multi-disc sorption bed. (a) disc-shaped sorbent packets; (b) fixing net; (c) heat exchanger main body.

2.2. Inlet/Outlet Manifolds

In the subsequent stages of the implementation works, it was necessary to build a lab-scale prototype of the multi-disc sorption bed. The crucial step in this stage was to design the inlet/outlet manifolds of cooling/heating water in order to incorporate the heat exchanger into the operational test stand. Therefore, three variants of the inlet/outlet manifold geometry depicted in Figure 3 have been investigated with the use of numerical methods.

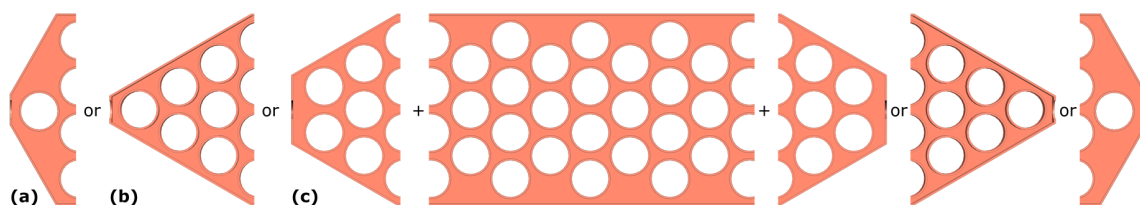


Figure 3. Variants of investigated inlet/outlet manifolds. (a–c) represent three variants of the inlet/outlet manifold geometry.

The most uniform spatial distribution of heating medium velocity within the main part of the multi-disc sorption bed and the largest temperature difference between inlet and outlet was obtained with variant (a) depicted in Figure 3 and therefore this inlet/outlet manifold geometry was used in the lab-scale prototype of the device for further analysis.

2.3. Lab-Scale Prototype

The physical prototype of the multi-disc sorption bed depicted in Figure 4 was constructed in the lab-scale. The detailed dimensions of the prototype are shown in Figure 5.

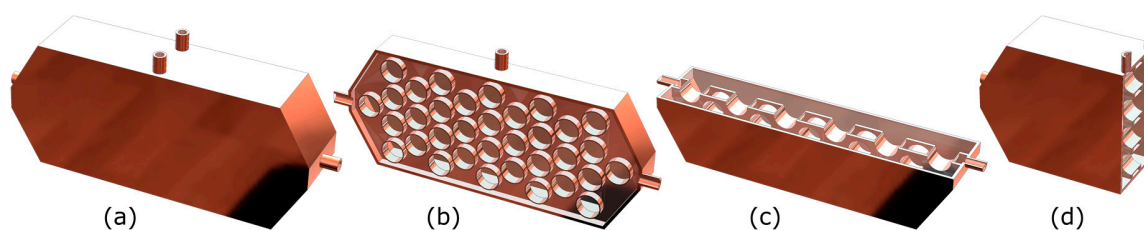


Figure 4. The prototype of the multi-disc sorption bed. (a) 3D view; (b–d) cross-section views.

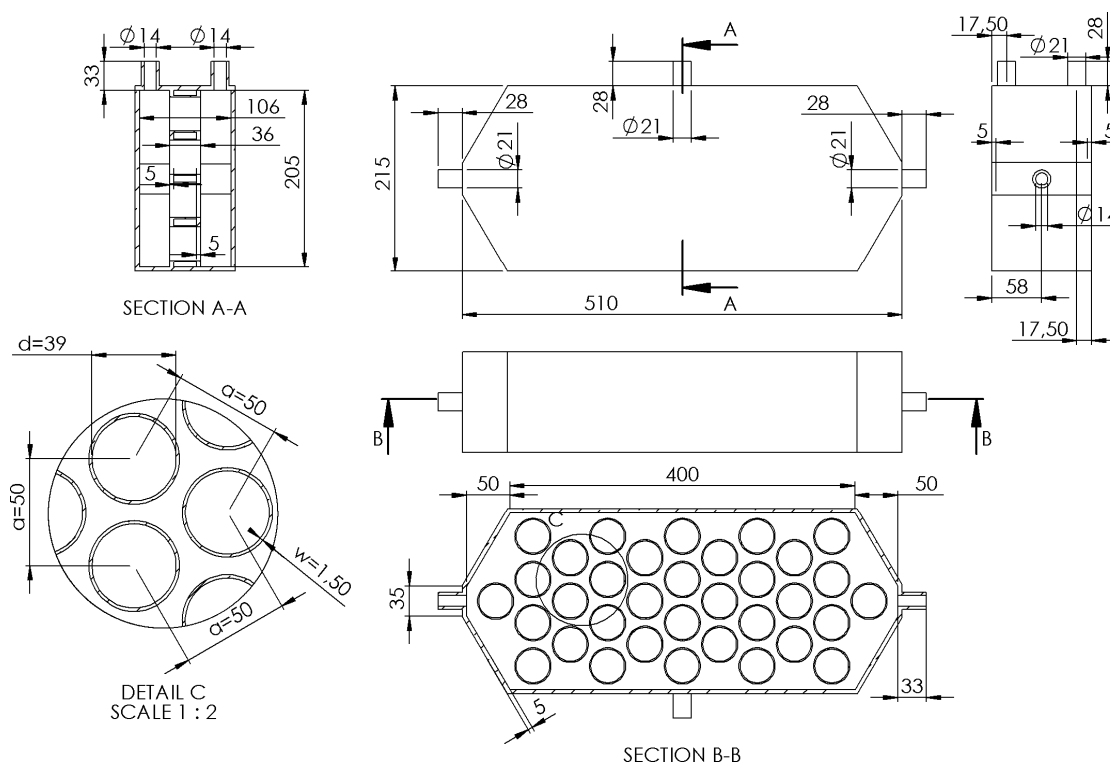


Figure 5. The dimensions (in mm) of the multi-disc sorption bed prototype.

The multi-disc sorption bed prototype is made of copper and the design allows to deliver water liquid, water vapor, or any other fluid medium through the connecting pipes to the two separate and water-tight volumes. The sorbent can be placed in the 34 disc-shaped packets and is secured with the fixing net (not shown in Figures 4 and 5).

3. Research Methods

3.1. Experimental Research

In the first stage of the research, the physical prototype of the multi-disc sorption bed was experimentally tested as a water–water heat exchanger in order to evaluate its heat transfer efficiency not being influenced by the sorption processes. Therefore, it was connected to the hot water supply of adjustable temperature and an open loop of cold water supply as depicted in Figure 6.

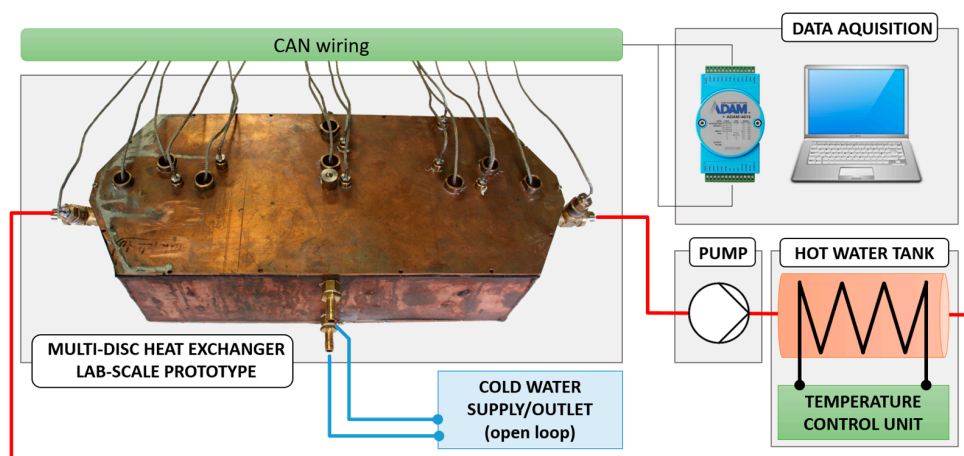


Figure 6. The experimental setup.

The prototype was equipped with PT-100 two-wire temperature sensors, with the measuring range of -50 to $+150$ K and the measuring accuracy of ± 0.1 K. The measuring probes were installed in the selected packets as well as outside the packets in the water jacket of the bed as depicted in Figure 7. The additional probes were installed in the inlets and outlets of both hot and cold water supplies.

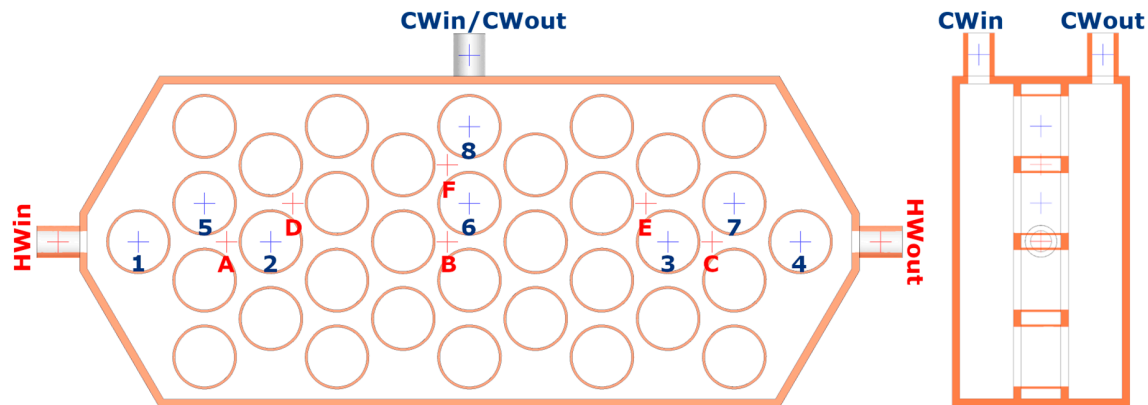


Figure 7. The temperature measuring points: A–F—hot water probes; 1–8—cold water probes.

The ADAM-4015 RTD module manufactured by Advantech was used to acquire the temperature values from individual measurement points with a frequency of 1 Hz. The turbine water flow meters of the measurement range of 0.008 – 0.2 dm³/s and the measurement accuracy of $\pm 2\%$ were used in order to determine the mass flow rate of both hot and cold water.

3.2. Numerical Research

3.2.1. CFD Tool

The application of numerical simulation tools calibrated with experimental measurements is a practical and cost-effective approach for energy simulation analysis [59]. CFD is the valuable simulation tool for the design of adsorption cooling systems and many researchers report the potential of using validated simulation models to investigate the performance of adsorption chillers [12]. CFD has been successfully applied in numerous research concerning conjugate heat transfer [53] as well as adsorption cooling and desalination technology [18,37]. Moreover, CFD allows for rapid prototyping and reliable analysis of several design configurations. The significance of CFD and the scope of its application have been increasing because of the rapid development of high-performance computing as well as cloud computing. Therefore, the commercial CFD package, ANSYS Fluent 2019 R1, was applied to carry out the numerical research. Its algorithm constrains the mass conservation of the velocity field by solving a pressure equation derived from the continuity and momentum equations. The nonlinear and coupled governing equations are solved iteratively.

In addition, an in-house code enhancing the solver capabilities of modeling sorption processes and described in Section 3.2.4. was applied within the carried out research.

3.2.2. Computational Domain and Discretization

The associative CAD model corresponding to the physical prototype of the multi-disc sorption bed was developed within the research. The model was parametrized and served as an input for the mesh generator.

In the first stage of the research, the prototype was tested as a water–water heat exchanger in order to validate the CFD model and therefore it consisted of three subdomains representing one solid region (copper multi-disc sorption bed) and two fluid regions (hot water and cold water). In the second stage, apart from the heat transfer and flow processes, the sorption phenomenon in the multi-disc bed was modeled using the developed in-house code. For that reason, the computational domain was modified

in order to take into account the sorbent and consisted of two solid regions (copper multi-disc sorption bed, disc-shaped sorbent packets) and two fluid regions (water, water vapor) as depicted in Figure 8.

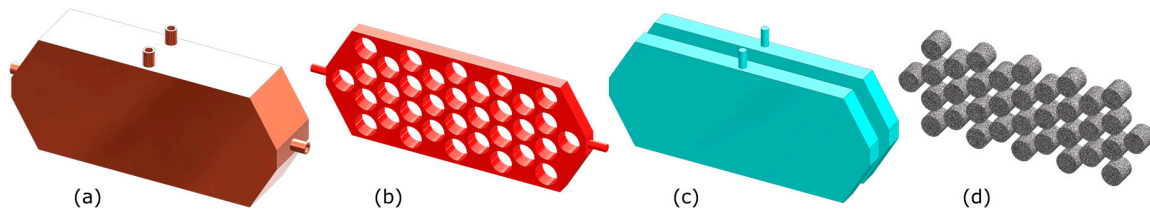


Figure 8. The computational domain consisting of four subdomains. (a) Multi-disc sorption bed; (b) water; (c) water vapor; (d) sorbent.

The accuracy and solution time are the two critical issues in CFD and both are highly dependent on the computational domain discretization. Different types of mesh elements are needed to deliver optimal performance in resolving different geometries and flow regimes [60]. Therefore, the MOSAIC[®] meshing was implemented in order to maintain the layered elements on the boundary layers and fill the rest of the volume with high-quality polyhedral elements (Figure 9). Polyhedral cells consume less memory and computing time in comparison to tetrahedral elements. Moreover, they also have many neighbors, so gradients can be better approximated and layered polyhedral prisms can be applied on the boundaries to efficiently capture the boundary layer on no-slip walls. The mesh is fully conformal, which ensures that the nodes on both sides of the interface between fluid and solid regions match to each other. Such an approach assures no interpolation at the interface, which contributes to the reduction of computational time and ensures higher accuracy of the solution.

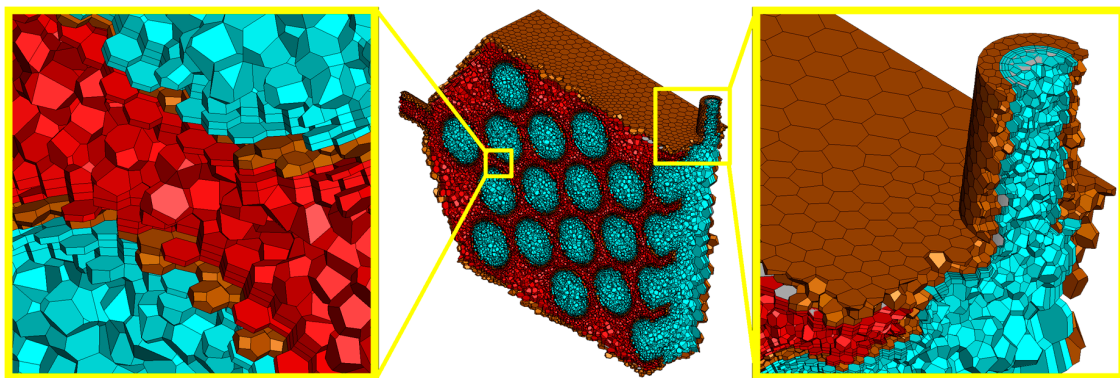


Figure 9. The computational domain discretization.

Mesh dependency studies based on the grid convergence index (*GCI*) were carried out in order to estimate the numerical accuracy resulting from the mesh resolution. The *GCI* is recommended by the Fluids Engineering Division of the American Society of Mechanical Engineers (ASME) to estimate the discretization error and was successfully applied in many research [61–64]. Three numerical meshes of different resolutions were generated for the analyzed geometry in order to estimate the discretization error with *GCI*.

The mean relative cell size was defined as the ratio of the average cell size h , defined in the Equation (1), and the characteristic dimension of the multi-disc sorption bed a , which is the distance between the centers of the two adjacent disc-shaped packets (Figure 5).

$$h = \sqrt[3]{\frac{1}{N} \sum_{i=1}^N (\Delta V_i)}, \quad (1)$$

where:

ΔV_i —volume of the i th cell;

N —total number of cells in the computational domain;

Initially, the mesh consisting of elements of mean relative cell size equal to 8.44×10^{-2} was generated and then meshes of mean relative cell sizes decreased to 6.46×10^{-2} and 4.72×10^{-2} were prepared by scaling the initial mesh.

The GCI was calculated in order to minimize the discretization error according to the procedure described in [65]. The grid refinement factor r (2) was calculated based on the representative mesh size h (1) as:

$$r = \frac{h_{coarse}}{h_{fine}}, \quad (2)$$

Moreover, the following assumption was made:

$$h_1 < h_2 < h_3; r_{21} = \frac{h_2}{h_1}; r_{32} = \frac{h_3}{h_2}, \quad (3)$$

The order of convergence p was calculated based on Equation (4) [65]:

$$p = \frac{\left| \ln \left| \frac{\varepsilon_{32}}{\varepsilon_{21}} \right| + \ln \left(\frac{r_{21}^p - 1 \cdot \operatorname{sgn} \left(\frac{\varepsilon_{32}}{\varepsilon_{21}} \right)}{r_{32}^p - 1 \cdot \operatorname{sgn} \left(\frac{\varepsilon_{32}}{\varepsilon_{21}} \right)} \right) \right|}{\ln(r_{21})}, \quad (4)$$

where:

$$\varepsilon_{32} = \phi_3 - \phi_2; \varepsilon_{21} = \phi_2 - \phi_1, \quad (5)$$

ϕ_k denotes the value of the variable important to the objective of the simulation study for the solution obtained with the k th mesh. The logarithmic mean temperature difference ($LMTD$) was selected as the above-mentioned variable.

The approximate relative error was calculated on the basis of Equation (6).

$$e_a^{21} = \left| \frac{\phi_1 - \phi_2}{\phi_1} \right| \quad (6)$$

Finally, the GCI was determined using Equation (7) provided in [65]:

$$GCI_{21} = \frac{1.25 \cdot e_a^{21}}{r_{21}^p - 1} \quad (7)$$

All the values of the above-defined quantities are listed in Table 1. The obtained results indicate the mesh convergence with the GCI equal to 1.03%.

Table 1. Mesh parameters and values of quantities calculated based on Equations (1)–(7).

h/a (-)	N (-)	$LMTD$ (K)	H (-)	R (-)	ε (-)	$\varepsilon_{i+1}/\varepsilon_i$ (-)	P (-)	e_a (%)	GCI (%)
$4.7 \cdot 10^{-2}$	888 694	25.84	2.3603	1.3680	-0.31				
$6.5 \cdot 10^{-2}$	347 133	25.53	3.2289	1.3067	-0.10	converged	2.867	1.20%	1.03%
$8.4 \cdot 10^{-2}$	155 590	25.43	4.2192	-	-				

3.2.3. Boundary Conditions and Model Settings

The first stage of numerical investigations aimed to validate the multi-disc sorption bed model operating as a water-water heat exchanger with the obtained experimental data. The heat transfer efficiency of the prototype was tested under three different R_{MFR} ratios defined with Equation (8)

and equal to 1.00, 1.33, and 1.66. The cold water inlet temperature was 294.1 K and hot water inlet temperature was 336.2 K. The above data was defined based on the experimental research.

$$R_{MFR} = \frac{\dot{m}_{HW}}{\dot{m}_{CW}}, \quad (8)$$

where:

\dot{m}_{HW} —hot water mass flow rate (kg/s);

\dot{m}_{CW} —cold water mass flow rate (kg/s);

In the second stage of the research, apart from the heat transfer and flow processes, the desorption process was investigated as the analysis of temperatures inside the bed during the desorption is important to show the spatial distributions of the main parameters of the chiller [2]. The boundary conditions corresponded with the final stage of the desorption phase of the adsorption chiller working cycle, therefore, the water of 343 K was the heating fluid and the mass-flow-inlet boundary condition of mass flow rate equal to 0.005 kg/s was assigned. The pressure-outlet boundary condition was defined on the outlet from the heating water subdomain. The heat transfer between fluid and solid subdomains was calculated as conjugate heat transfer. Parameters of the applied materials are defined in Table 2.

Table 2. Materials parameters.

Material	Density (kg·m ⁻³)	Specific Heat (J·kg ⁻¹ ·K ⁻¹)	Thermal Cond. (W·m ⁻¹ ·K ⁻¹)	Viscosity (kg·m ⁻¹ ·s ⁻¹)
water (liquid)	998.2	4182	0.6	1.003·10 ⁻³
water (vapor)	0.5542	f(T)	0.0261	1.34·10 ⁻⁵
silica gel	800	924	0.18	-
copper	8978	381	387.6	-

The CFD solver was configured as pressure-based and the analysis was performed for a steady state. The standard *k-ε* viscous model was applied along with the enhanced wall treatment. Pressure–velocity coupling by the COUPLED algorithm was used as a solution method. Least squares cell-based spatial discretization was chosen in case of gradients, second order in case of pressure, second-order upwind in case of momentum, as well as energy and first-order upwind in case of turbulent dissipation rate. The model convergence was defined on the basis of qualitative and quantitative monitoring of residuals as well as the thermodynamic stability of the model. The developed in-house model described in the next subsection was used in order to model the sorption phenomenon.

3.2.4. Sorption Modeling

The commercial ANSYS Fluent tool used in this research, dedicated to CFD analysis, does not allow for sufficient consideration of the aspects related to heat and mass exchange during sorption processes. Therefore, it was necessary to expand the available models by using the in-house algorithm implemented as a user-defined functions (UDF). The algorithm developed within the research constitutes a novelty in 3D modelling of the sorption processes in adsorption cooling technology. The UDF created within the framework of this research is a program written in the C programming language. In order to effectively incorporate it into the solver code, it was developed using the Microsoft Visual Studio compiler. It was decided to use the compiled UDF because compared to the interpreted UDF, it is characterized by faster operation, no limitation on the programming language, the ability to call functions written in other programs, and the ability to run executable files. Especially the first of the above-mentioned features, i.e., faster operation, was crucial for the choice of the UDF type.

Numerical modeling of sorption processes requires an extensive approach to mathematical description of heat exchange in a sorbent bed, as it is necessary to take into account the fluctuations in the local intensity of heat production or consumption during the exothermic adsorption or endothermic

desorption process, respectively. The above-mentioned intensity of heat production or consumption in the bed depends directly on the local temperature of the sorbent, which in turn is closely correlated with the design and operating parameters of the heat exchanger. In order to take these factors into account in the model, it was decided to modify the source term in the energy equation. The source term enables to describe the exo- and endothermic character of sorption processes and, more importantly, their two-way coupling with the thermal-flow field calculated by the solver.

The intensity of sorption processes in the developed model depends on the local temperature of the sorbent by the function allowing to generate the temperature value in a given numerical mesh element by the solver's algorithm. Then the heat source is calculated as a function of the intensity of sorption depending on the local temperature obtained in the first step. Subsequently, the derivative of the heat source with respect to temperature is calculated and the value of the volumetric heat source is assigned to the function returned to the algorithm of the solver.

The mathematical dependence of the sorption intensity and the sorbent temperature was determined as a polynomial function of coefficients defined and validated during previous studies concerning heat transfer in the sorption beds [18,37].

4. Results and Discussion

4.1. Heat Transfer Efficiency

The logarithmic mean temperature difference (*LMTD*) defined in Equation (9) is the average temperature difference between the hot and cold fluids [66] and therefore it was used to determine the efficiency of the multi-disc sorption bed operating as a crossflow water–water heat exchanger.

$$LMTD = \frac{\Delta T_{inlet} - \Delta T_{outlet}}{\ln\left(\frac{\Delta T_{inlet}}{\Delta T_{outlet}}\right)} = \frac{(HW_{in} - CW_{in}) - (HW_{out} - CW_{out})}{\ln\left(\frac{HW_{in} - CW_{in}}{HW_{out} - CW_{out}}\right)}, \quad (9)$$

where:

HW_{in} —hot water inlet temperature (K);

HW_{out} —hot water outlet temperature (K);

CW_{in} —cold water inlet temperature (K);

CW_{out} —cold water outlet temperature (K);

According to [66], the *LMTD* calculated for the crossflow heat exchanger has to be corrected with the factor *F* read from the graph presented in [66] (page 52) and based on the coefficients *P* and *R* defined in Equation (10).

$$P = \frac{CW_{out} - CW_{in}}{HW_{in} - CW_{in}}, \quad R = \frac{HW_{in} - HW_{out}}{CW_{out} - CW_{in}}, \quad (10)$$

The *LMTD*, *P*, *R*, *F*, and corrected *LMTD* for the multi-disc sorption bed operating as a crossflow water–water heat exchanger calculated based on both the experimental and CFD results for the analyzed R_{MFR} are presented in Table 3. The correction factor *F* is close to 1 for all analyzed R_{MFR} ratios, which indicate the very good efficiency of the investigated innovative multi-disc construction.

Table 3. The obtained logarithmic mean temperature difference (*LMTD*), *P*, *R*, *F*, and corrected *LMTD* values.

Analyzed Case	<i>LMTD</i> (K)	<i>P</i> (-)	<i>R</i> (-)	<i>F</i> (-)	<i>F</i> × <i>LMTD</i> (K)
$R_{MFR} = 1.00$; EXP	27.19	0.306	1.000	0.975	26.51
$R_{MFR} = 1.00$; CFD	25.84	0.326	1.017	0.970	25.07
$R_{MFR} = 1.33$; EXP	27.47	0.340	0.776	0.985	27.06
$R_{MFR} = 1.33$; CFD	26.70	0.361	0.742	0.985	26.30
$R_{MFR} = 1.66$; EXP	28.23	0.363	0.588	0.985	27.80
$R_{MFR} = 1.66$; CFD	27.16	0.384	0.598	0.980	26.62

The temperatures obtained during the experimental research were compared with the CFD results in order to validate the numerical model (Figure 10). Along with the increase of the R_{MFR} , the temperatures also increased on both the hot and cold side of the sorption bed operating as a water–water heat exchanger. The lowest temperature was recorded by Probe 8 for all the analyzed R_{MFR} ratios, although CFD results were 2.0% ($R_{MFR} = 1.00$ and 1.33) or 2.1% ($R_{MFR} = 1.66$) higher in comparison to experimental results. The highest temperature was recorded by Probe A for all the analyzed R_{MFR} ratios. The relative difference between CFD and experimental results for Probe A ranged between 0.6% to 1.2%. The CFD and experimental results are qualitatively similar. The quantitative differences are presented in Figure 11 and range from 0.6% to 7.0%.

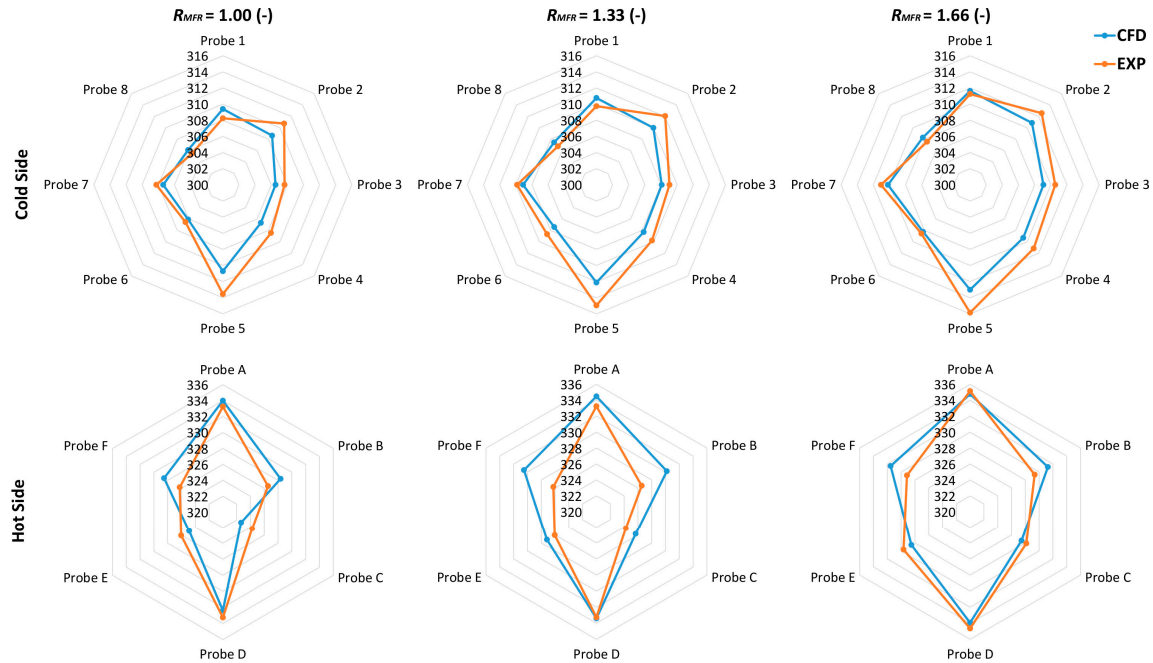


Figure 10. The temperatures in the multi-disc sorption bed operating as a water–water heat exchanger obtained within the experimental research and computational fluid dynamics (CFD) analysis.

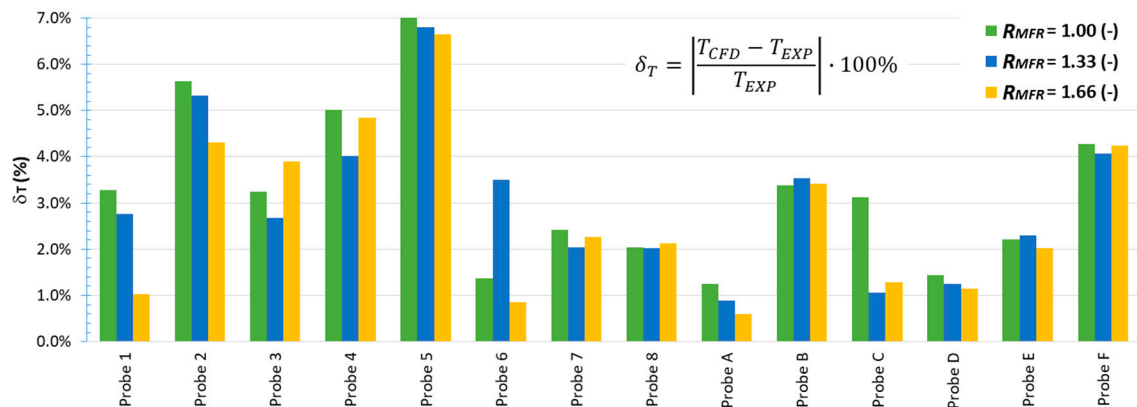


Figure 11. The relative difference between the temperatures in the multi-disc sorption bed operating as a water–water heat exchanger obtained in the experimental research and CFD analysis.

4.2. Temperature Field in the Sorption Bed

In the second stage of the research, the silica gel was placed into the disc-shaped packets in order to simulate the spatial distribution of temperature in the sorption bed at the end of the desorption cycle. The CFD analysis was performed for five d/a ratios, where d represents the inner diameter of the disc-shaped packet and a is the distance between the centers of the two adjacent packets.

The temperature along the line extending through the sorption bed from the water inlet (relative length = 0) to the water outlet (relative length = 1) is presented in Figure 12. Figures 13–17 present the temperature fields in the cross-sections of the sorption bed for all the analyzed d/a ratios (0.54, 0.62, 0.70, 0.78, and 0.86). The above-mentioned figures indicate that the temperature drop within the sorbent packets strongly depends on the d/a ratio. The lowest temperature in the center of the sorbent packet was approx. 312 K in the case of $d/a = 0.54$ and the highest temperature was approx. 325 K in the case of $d/a = 0.86$. The average sorbent temperature, as well as the temperature distribution in the bed, is highly influenced by the d/a ratio. The temperature distribution in the bed is the result of the superposition of the heat transferred from the heating water as well as the thermal characteristics of sorption kinetics. The proposed multi-disc sorption bed design is beneficial in terms of the spatial temperature distribution in the bed.

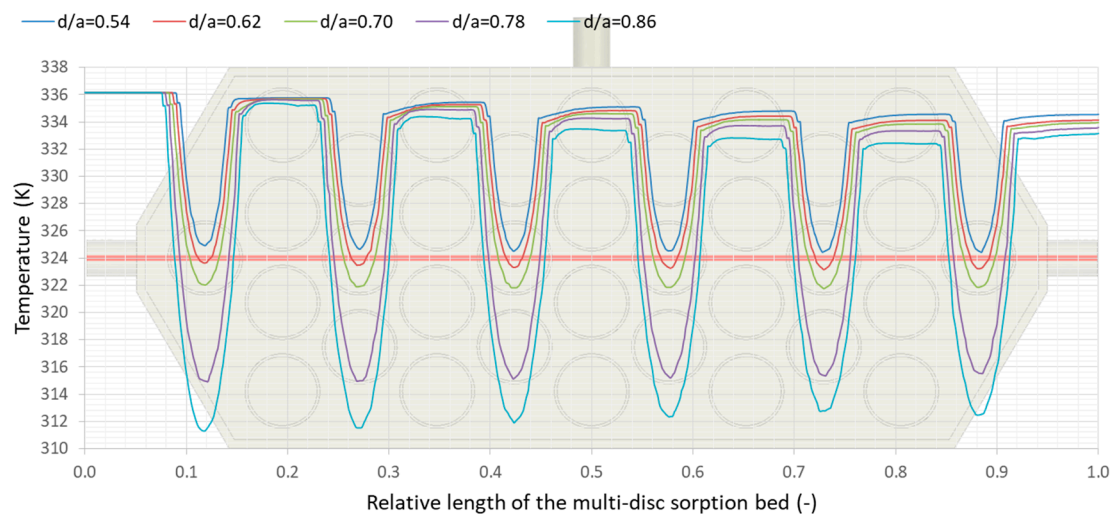


Figure 12. The temperature along the centerline of the sorption bed extending from the inlet (relative length = 0) to the outlet (relative length = 1).

The temperature drop within the sorbent entails the differences of the hot water temperature gradients (ΔT_{HW}) in the sorption bed presented in Table 4. The ΔT_{HW} is directly proportional to the heating power (HP) defined in Equation (11), which is one of the most important parameters of the adsorption chiller. Therefore, the increase in ΔT_{HW} obtained through the analyzed cases leads to a 69% increase in HP for constant mass flow rate (\dot{m}_{HW}) and specific heat (c_p) of heating water.

$$HP = \dot{m}_{HW} \cdot c_p \cdot \Delta T_{HW}, \quad (11)$$

On the other hand, the increased d/a ratio induces a higher pressure drop in the sorbent bed, which entails higher electricity consumption to power the hot water pump. This directly indicates the d/a ratio as the crucial parameter, which has to be considered in the design of the multi-disc sorption bed and properly balanced according to the specific requirements of the installation site.

Table 4. The hot water temperature (ΔT_{HW}) for all d/a ratios and the relative increase in heating power ($HP\%$) as well as hot water pressure drop ($\Delta p_{HW\%}$) in relation to the $d/a = 0.54$.

d/a (-)	0.54	0.62	0.70	0.78	0.86
ΔT_{HW} (K)	1.71	2.10	2.24	2.52	2.89
$HP\%$ (%)	0	23	31	47	69
$\Delta p_{HW\%}$ (%)	0	2	5	12	43

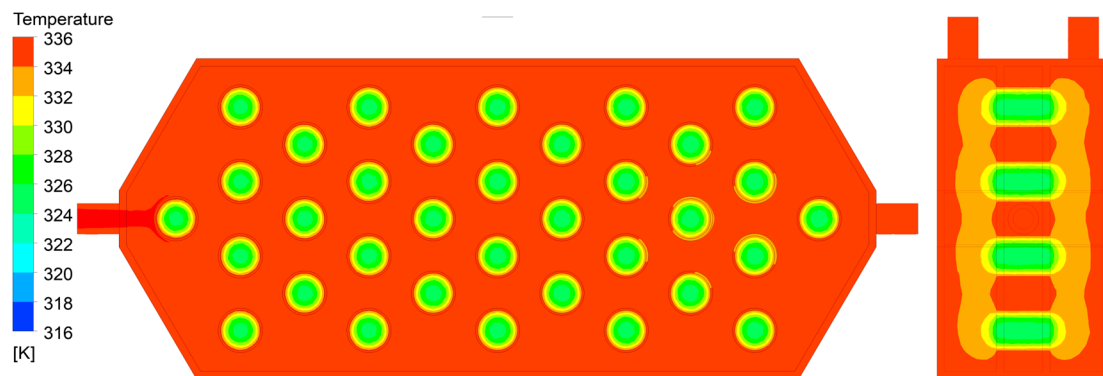


Figure 13. Temperature field in the cross-sections of the multi-disc sorption bed for $d/a = 0.54$.

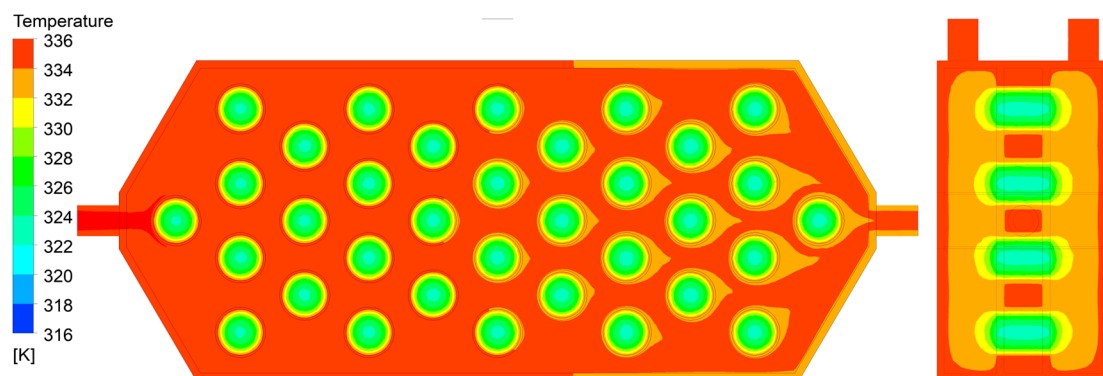


Figure 14. Temperature field in the cross-sections of the multi-disc sorption bed for $d/a = 0.62$.

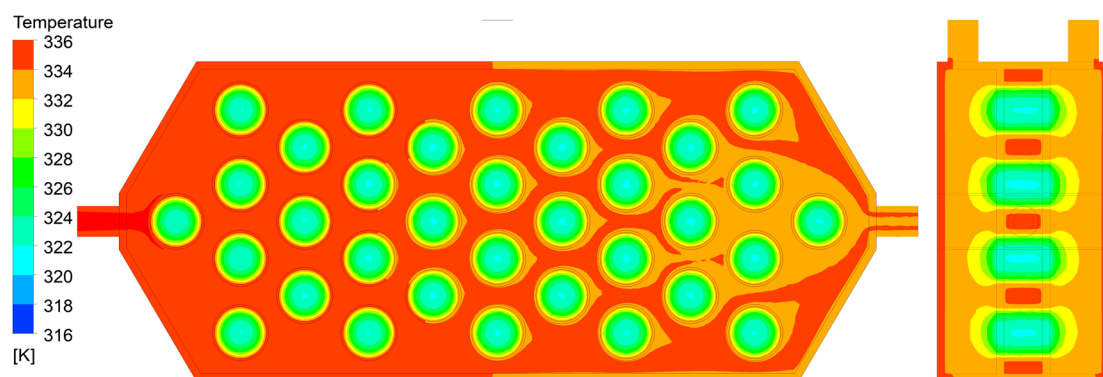


Figure 15. Temperature field in the cross-sections of the multi-disc sorption bed for $d/a = 0.70$.

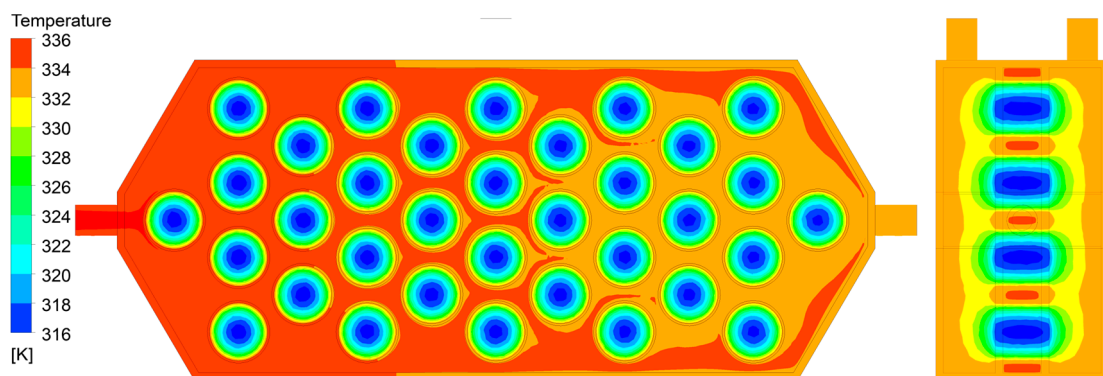


Figure 16. Temperature field in the cross-sections of the multi-disc sorption bed for $d/a = 0.78$.

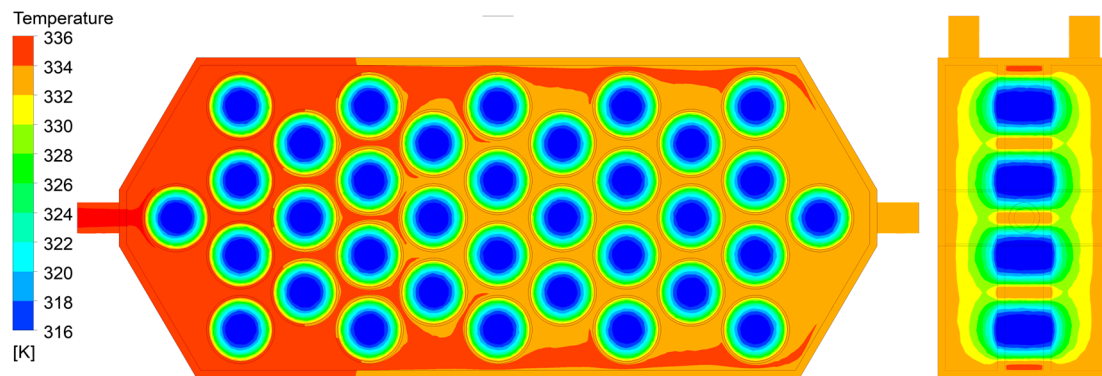


Figure 17. Temperature field in the cross-sections of the multi-disc sorption bed for $d/a = 0.86$.

The thickness of the copper wall of the disc-shaped packets was 1.5 mm for all the analyzed cases. The preliminary analysis revealed its insignificant influence on the temperature distribution in the bed. Such behavior results from the very high thermal conductivity of copper in comparison to the thermal conductivity of silica gel or water. Therefore, the wall thickness of the packets should be defined on the basis of mechanical analysis of the sorption bed rigidity while keeping in mind the requirement of minimizing both the bed mass and material cost.

4.3. Weight and Dimension Factors

The adsorption chiller performance is directly influenced by the thermal parameters, but the weight and dimensions of the sorption beds are, in some cases, the factors limiting the widespread application of the adsorption cooling technology. Therefore, the proper balance between the sorbent and metal in the sorption bed has to be thoroughly investigated.

One of the factors presenting the balance between the metal and the sorbent is the heat exchanger mass to sorbent ratio ($R_{HX/S}$) defined as the quotient of the total mass of the cylindrical heat transfer walls of the heat exchanger (m_{HX}) to the total sorbent mass (m_s). Lower values of $R_{HX/S}$ ratio are desirable in terms of the adsorption chiller performance and compact dimensions. Moreover, decreasing the fraction of heat exchanger mass in the total mass of the device leads to the growth of the COP because of supplying a greater portion of the thermal energy to the sorbent itself and not to the metal part of the sorption bed. Therefore, the d/a equal to 0.86 is the most advantageous design parameter value in the above context.

The ratio of heat transfer surface (S) to the sorbent mass (m_s) is convenient to assess the degree of a dynamic perfection of the sorption bed as it is proportional to the specific power; the larger the ratio the higher power per unit adsorbent mass can be obtained [32].

Both indicators for all the analyzed d/a ratios are depicted in Figure 18 and both decrease along with the increase of the d/a ratio.

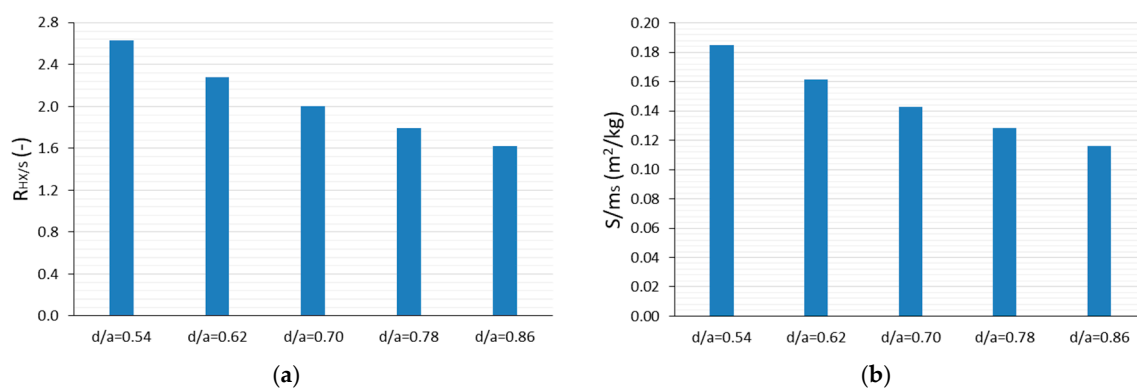


Figure 18. The influence of multi-disc sorption bed design on $R_{HX/S}$ (a) and S/m_s (b) ratios.

5. Conclusions

The paper presents the analysis concerning the application of the multi-disc sorption bed of the adsorption chillers designed for chill and desalinated water production. The heat exchanger is the crucial element of the device because of its fundamental influence on the chiller performance indicators such as heating power (*HP*) or the coefficient of performance (*COP*). Moreover, it highly impacts the mass and dimensions of the sorption bed, and these factors are critical for the widespread utilization of the adsorption technology. The proposed multi-disc sorption bed contributes to the increase of heat transfer surface area and simultaneously assures a compact and lightweight design of the device. The developed design allows to place the device e.g., in the ceiling of the building or integrate it with solar panels, which will supply the device with the necessary heat. Such a solution allows to significantly expand the potential installation sites of the adsorption chillers and thus reduce one of the main disadvantages of these devices, which is the need to dedicate a large space for the installation of the adsorption chiller. Another advantage of the proposed construction is its potential for scalability consisting of adjusting the number of sorbent discs to the expected cooling capacity of the device or the possibility of installing two or more multi-disc sorption beds with sorbent packages one above another with the space between them being a vapor collector.

There is a great interest in the numerical modeling of adsorption chillers and particularly the sorption beds. However, the majority of the available models are characterized by significant limitations and only few of them are three-dimensional ones. Furthermore, some of the models presented in the literature are not experimentally validated and simulate only the packed bed not taking the heat exchanger geometry into consideration. Therefore, the developed and validated in-house algorithm allowing to model sorption along with thermal and flow processes in the 3D numerical model of the whole sorption bed filled the above-mentioned gap. The model takes into account the conjugate heat transfer as well as the thermal characteristics of the sorption phenomenon. In consequence, the developed model can contribute to the improvement of the design of adsorption beds by the capability of optimizing the sorption bed performance and geometry.

The CFD analysis performed with the use of the developed model incorporated into the commercial CFD code allowed to define the design of the investigated type of the sorption bed and its correlation with basic factors influencing the performance and dimensions of the sorption bed, such as gradient of heating water temperature (ΔT_{HW}), logarithmic mean temperature difference (*LMTD*), heat exchanger mass to sorbent ratio ($R_{HX/S}$), and heat transfer surface to sorbent mass ratio (S/m_s).

Funding: This research was funded by the National Science Centre of the Republic of Poland, grant number 2018/29/B/ST8/00442. The APC was funded by Ministry of Science and Higher Education of the Republic of Poland, grant number 944/P-DUN/2019.

Conflicts of Interest: The author declares no conflict of interest. The funders had no role in the design of the study; in the collection, analyses, or interpretation of data; in the writing of the manuscript, or in the decision to publish the results.

References

1. Alsaman, A.; Askalany, A.; Ahmed, M.; Ali, E.; Harby, K.; Diab, M. Simulation model for silica gel-water adsorption cooling system powered by renewable energy. In Proceedings of the 3rd International Conference on Energy Engineering Faculty, of Energy Engineering, Aswan University, Aswan, Egypt, 28–30 December 2015.
2. Elsheniti, M.B.; Hassab, M.A.; Attia, A.-E. Examination of effects of operating and geometric parameters on the performance of a two-bed adsorption chiller. *Appl. Therm. Eng.* **2018**, *146*, 674–687. [[CrossRef](#)]
3. Sultana, T. Effect of overall thermal conductance with different mass allocation on a two stage adsorption chiller employing re-heat scheme. Master's Thesis, Bangladesh University of Engineering and Technology, Dhaka, Bangladesh, 2008.

4. Khan, M.Z.I.; Alam, K.; Saha, B.B.; Hamamoto, Y.; Akisawa, A.; Kashiwagi, T. Parametric study of a two-stage adsorption chiller using re-heat—The effect of overall thermal conductance and adsorbent mass on system performance. *Int. J. Therm. Sci.* **2006**, *45*, 511–519. [\[CrossRef\]](#)
5. Saha, B.B.; Koyama, S.; Kashiwagi, T.; Akisawa, A.; Ng, K.C.; Chua, H.T. Waste heat driven dual-mode, multi-stage, multi-bed regenerative adsorption system. *Int. J. Refrig.* **2003**, *26*, 749–757. [\[CrossRef\]](#)
6. Sur, A.; Das, R.K. Review of technology used to improve heat and mass transfer characteristics of adsorption refrigeration system. *Int. J. Air Cond. Refrig.* **2016**, *24*, 1630003. [\[CrossRef\]](#)
7. Hassan, H.; Mohamad, A.; Alyousef, Y.; Al-Ansary, H. A review on the equations of state for the working pairs used in adsorption cooling systems. *Renew. Sustain. Energy Rev.* **2015**, *45*, 600–609. [\[CrossRef\]](#)
8. Voyiatzis, E.; Stefanakis, N.; Palyvos, J.; Papadopoulos, A. Computational study of a novel continuous solar adsorption chiller: Performance prediction and adsorbent selection. *Int. J. Energy Res.* **2007**, *31*, 931–946. [\[CrossRef\]](#)
9. Sztékler, K.; Kalawa, W.; Stefanski, S.; Krzywanski, J.; Grabowska, K.; Sosnowski, M.; Nowak, W. The influence of adsorption chillers on CHP power plants. *MATEC Web Conf.* **2018**, *240*, 05033. [\[CrossRef\]](#)
10. Sztékler, K.; Kalawa, W.; Nowak, W.; Stefanski, S.; Krzywanski, J.; Grabowska, K. Using the adsorption chillers for waste heat utilisation from the CCS installation. *EPJ Web Conf.* **2018**, *180*, 02106. [\[CrossRef\]](#)
11. Sztékler, K.; Kalawa, W.; Nowak, W.; Stefanski, S.; Krzywanski, J.; Grabowska, K. Using the adsorption chillers for utilisation of waste heat from rotary kilns. *EPJ Web Conf.* **2018**, *180*, 02105. [\[CrossRef\]](#)
12. Rezk, A.; Al-Dadah, R.; Mahmoud, S.; Elsayed, A. Effects of contact resistance and metal additives in finned-tube adsorbent beds on the performance of silica gel/water adsorption chiller. *Appl. Therm. Eng.* **2013**, *53*, 278–284. [\[CrossRef\]](#)
13. Saravanan, R.; Maiya, M.P. Thermodynamic comparison of water-based working fluid combinations for a vapour absorption refrigeration system. *Appl. Therm. Eng.* **1998**, *18*, 553–568. [\[CrossRef\]](#)
14. Kurniawan, A.; Rachmat, A. Others CFD Simulation of Silica Gel as an Adsorbent on Finned Tube Adsorbent Bed. *E3S Web Conf.* **2018**, *67*, 01014. [\[CrossRef\]](#)
15. Pyrka, P. Modelowanie trójzłożowej chłodziarki adsorpcyjnej. *Zesz. Energetyczne* **2014**, *1*, 205–216.
16. White, J. Literature review on adsorption cooling systems. *Lat. Am. Caribb. J. Eng. Educ.* **2013**. Available online: https://www.researchgate.net/publication/289127089_LITERATURE_REVIEW_ON_ADSORPTION_COOLING_SYSTEMS (accessed on 8 December 2019).
17. Shahzad, M.W.; Ybyraiymkul, D.; Burhan, M.; Oh, S.J.; Ng, K.C. An innovative pressure swing adsorption cycle. *AIP Conf. Proc.* **2019**, *2062*, 020057.
18. Grabowska, K.; Sosnowski, M.; Krzywanski, J.; Sztékler, K.; Kalawa, W.; Zylka, A.; Nowak, W. The Numerical Comparison of Heat Transfer in a Coated and Fixed Bed of an Adsorption Chiller. *J. Therm. Sci.* **2018**, *27*, 421–426. [\[CrossRef\]](#)
19. Xu, S.Z.; Wang, L.W.; Wang, R.Z. Thermodynamic analysis of single-stage and multi-stage adsorption refrigeration cycles with activated carbon–ammonia working pair. *Energy Convers. Manag.* **2016**, *117*, 31–42. [\[CrossRef\]](#)
20. Starace, G.; Fiorentino, M.; Meleleo, B.; Risolo, C. The hybrid method applied to the plate-finned tube evaporator geometry. *Int. J. Refrig.* **2018**, *88*, 67–77. [\[CrossRef\]](#)
21. Fiorentino, M.; Starace, G. The design of countercurrent evaporative condensers with the hybrid method. *Appl. Therm. Eng.* **2018**, *130*, 889–898. [\[CrossRef\]](#)
22. Elsheniti, M.B.; Elsamni, O.A.; Al-dadah Raya, K.; Mahmoud, S.; Elsayed, E.; Saleh, K. Adsorption refrigeration technologies. In *Sustainable Air Conditioning Systems*; BoD—Books on Demand: Norderstedt, Germany, 2018.
23. Wu, W.-D.; Zhang, H.; Men, C. Performance of a modified zeolite 13X-water adsorptive cooling module powered by exhaust waste heat. *Int. J. Therm. Sci.* **2011**, *50*, 2042–2049. [\[CrossRef\]](#)
24. Sakoda, A.; Suzuki, M. Fundamental study on solar powered adsorption cooling system. *J. Chem. Eng. Jpn.* **1984**, *17*, 52–57. [\[CrossRef\]](#)
25. Sakoda, A.; Suzuki, M. Simultaneous Transport of Heat and Adsorbate in Closed Type Adsorption Cooling System Utilizing Solar Heat. *J. Sol. Energy Eng. Trans. Asme. J. Sol. Energy Eng.* **1986**, *108*, 239–245. [\[CrossRef\]](#)
26. Bahrehmand, H.; Khajepour, M.; Bahrami, M. Finding optimal conductive additive content to enhance the performance of coated sorption beds: An experimental study. *Appl. Therm. Eng.* **2018**, *143*, 308–315. [\[CrossRef\]](#)

27. Kim, D.-S.; Chang, Y.-S.; Lee, D.-Y. Modelling of an adsorption chiller with adsorbent-coated heat exchangers: Feasibility of a polymer-water adsorption chiller. *Energy* **2018**, *164*, 1044–1061. [\[CrossRef\]](#)
28. Li, A.; Thu, K.; Ismail, A.B.; Shahzad, M.W.; Ng, K.C. Performance of adsorbent-embedded heat exchangers using binder-coating method. *Int. J. Heat Mass Transf.* **2016**, *92*, 149–157. [\[CrossRef\]](#)
29. Grabowska, K.; Krzywanski, J.; Nowak, W.; Wesolowska, M. Construction of an innovative adsorbent bed configuration in the adsorption chiller-Selection criteria for effective sorbent-glue pair. *Energy* **2018**, *151*, 317–323. [\[CrossRef\]](#)
30. Chang, K.-S.; Chen, M.-T.; Chung, T.-W. Effects of the thickness and particle size of silica gel on the heat and mass transfer performance of a silica gel-coated bed for air-conditioning adsorption systems. *Appl. Therm. Eng.* **2005**, *25*, 2330–2340. [\[CrossRef\]](#)
31. Grabowska, K.; Sosnowski, M.; Krzywanski, J.; Sztékler, K.; Kalawa, W.; Zylka, A.; Nowak, W. Analysis of heat transfer in a coated bed of an adsorption chiller. *MATEC Web Conf.* **2018**, *240*, 01010. [\[CrossRef\]](#)
32. Aristov, Y.I.; Glaznev, I.S.; Gírník, I.S. Optimization of adsorption dynamics in adsorptive chillers: Loose grains configuration. *Energy* **2012**, *46*, 484–492. [\[CrossRef\]](#)
33. Askalany, A.A.; Henninger, S.K.; Ghazy, M.; Saha, B.B. Effect of improving thermal conductivity of the adsorbent on performance of adsorption cooling system. *Appl. Therm. Eng.* **2017**, *110*, 695–702. [\[CrossRef\]](#)
34. Gírník, I.S.; Aristov, Y.I. Making adsorptive chillers more fast and efficient: The effect of bi-dispersed adsorbent bed. *Appl. Therm. Eng.* **2016**, *106*, 254–256. [\[CrossRef\]](#)
35. Demir, H.; Mobedi, M.; Ülkü, S. Effects of porosity on heat and mass transfer in a granular adsorbent bed. *Int. Commun. Heat Mass Transf.* **2009**, *36*, 372–377. [\[CrossRef\]](#)
36. Alam, K.C.A.; Saha, B.B.; Kang, Y.T.; Akisawa, A.; Kashiwagi, T. Heat exchanger design effect on the system performance of silica gel adsorption refrigeration systems. *Int. J. Heat Mass Transf.* **2000**, *43*, 4419–4431. [\[CrossRef\]](#)
37. Sosnowski, M.; Grabowska, K.; Krzywanski, J.; Nowak, W.; Sztékler, K.; Kalawa, W. The effect of heat exchanger geometry on adsorption chiller performance. *J. Phys. Conf. Ser.* **2018**, *1101*, 012037. [\[CrossRef\]](#)
38. Hong, S.; Ahn, S.; Kwon, O.; Chung, J. Optimization of a fin-tube type adsorption chiller by design of experiment. *Int. J. Refrig.* **2015**, *49*, 49–56. [\[CrossRef\]](#)
39. Ilis, G.G.; Demir, H.; Mobedi, M.; Saha, B.B. A new adsorbent bed design: Optimization of geometric parameters and metal additive for the performance improvement. *Appl. Therm. Eng.* **2019**, *162*, 114270. [\[CrossRef\]](#)
40. Gong, L.; Wang, R.; Xia, Z.; Chen, C. Design and performance prediction of a new generation adsorption chiller using composite adsorbent. *Energy Convers. Manag.* **2011**, *52*, 2345–2350. [\[CrossRef\]](#)
41. Rogala, Z. Adsorption chiller using flat-tube adsorbers—Performance assessment and optimization. *Appl. Therm. Eng.* **2017**, *121*, 431–442. [\[CrossRef\]](#)
42. Çağlar, A. The effect of fin design parameters on the heat transfer enhancement in the adsorbent bed of a thermal wave cycle. *Appl. Therm. Eng.* **2016**, *104*, 386–393. [\[CrossRef\]](#)
43. Pajdak, A.; Kudasik, M.; Skoczylas, N.; Wierzbicki, M.; Braga, L.T.P. Studies on the competitive sorption of CO₂ and CH₄ on hard coal. *Int. J. Greenh. Gas Control* **2019**, *90*, 102789. [\[CrossRef\]](#)
44. Pajdak, A.; Skoczylas, N.; Dębski, A.; Grzegorek, J.; Maziarz, W.; Kudasik, M. CO₂ and CH₄ sorption on carbon nanomaterials and coals—Comparative characteristics. *J. Nat. Gas Sci. Eng.* **2019**, *72*, 103003. [\[CrossRef\]](#)
45. Intini, M.; Goldsworthy, M.; White, S.; Joppolo, C.M. Experimental analysis and numerical modelling of an AQSOA zeolite desiccant wheel. *Appl. Therm. Eng.* **2015**, *80*, 20–30. [\[CrossRef\]](#)
46. Gurgel, J.; Andrade Filho, L.; Grenier, P.; Meunier, F. Thermal diffusivity and adsorption kinetics of silica-gel/water. *Adsorption* **2001**, *7*, 211–219. [\[CrossRef\]](#)
47. Demir, H.; Mobedi, M.; Ülkü, S. A review on adsorption heat pump: Problems and solutions. *Renew. Sustain. Energy Rev.* **2008**, *12*, 2381–2403. [\[CrossRef\]](#)
48. Krzywanski, J.; Grabowska, K.; Sosnowski, M.; Zylka, A.; Sztékler, K.; Kalawa, W.; Wójcik, T.; Nowak, W. Modeling of a re-heat two-stage adsorption chiller by AI approach. *MATEC Web Conf.* **2018**, *240*, 05014. [\[CrossRef\]](#)
49. Krzywanski, J.; Grabowska, K.; Herman, F.; Pyrka, P.; Sosnowski, M.; Prauzner, T.; Nowak, W. Optimization of a three-bed adsorption chiller by genetic algorithms and neural networks. *Energy Convers. Manag.* **2017**, *153*, 313–322. [\[CrossRef\]](#)

50. Krzywanski, J.; Grabowska, K.; Sosnowski, M.; Zylka, A.; Sztekler, K.; Kalawa, W.; Wojcik, T.; Nowak, W. An adaptive neuro-fuzzy model of a re-heat two-stage adsorption chiller. *Therm. Sci.* **2019**, *23*, 1053–1063. [\[CrossRef\]](#)
51. Papakokkinos, G.; Castro, J.; López, J.; Oliva, A. A generalized computational model for the simulation of adsorption packed bed reactors—Parametric study of five reactor geometries for cooling applications. *Appl. Energy* **2019**, *235*, 409–427. [\[CrossRef\]](#)
52. Sosnowski, M. Computational domain discretization in numerical analysis of forced convective heat transfer within packed beds of granular materials. *Eng. Mech.* **2018**, *2018*, 801–804.
53. Sosnowski, M.; Krzywanski, J.; Grabowska, K.; Gnatowska, R. Polyhedral meshing in numerical analysis of conjugate heat transfer. *EPJ Web Conf.* **2018**, *180*, 02096. [\[CrossRef\]](#)
54. Sosnowski, M. Computational domain discretization in numerical analysis of flow within granular materials. *EPJ Web Conf.* **2018**, *180*, 02095. [\[CrossRef\]](#)
55. Sosnowski, M.; Gnatowska, R.; Sobczyk, J.; Wodziak, W. Numerical modelling of flow field within a packed bed of granular material. *J. Phys. Conf. Ser.* **2018**, *1101*, 012036. [\[CrossRef\]](#)
56. Mitra, S.; Oh, S.T.; Saha, B.B.; Dutta, P.; Srinivasan, K. Simulation study of the adsorption dynamics of cylindrical silica gel particles. *Heat Transf. Res.* **2015**, *46*, 123–140. [\[CrossRef\]](#)
57. Khan, M.Z.I.; Alam, K.C.A.; Saha, B.B.; Akisawa, A.; Kashiwagi, T. Study on a re-heat two-stage adsorption chiller—The influence of thermal capacitance ratio, overall thermal conductance ratio and adsorbent mass on system performance. *Appl. Therm. Eng.* **2007**, *27*, 1677–1685. [\[CrossRef\]](#)
58. Wang, R.Z.; Xia, Z.Z.; Wang, L.W.; Lu, Z.S.; Li, S.L.; Li, T.X.; Wu, J.Y.; He, S. Heat transfer design in adsorption refrigeration systems for efficient use of low-grade thermal energy. *Energy* **2011**, *36*, 5425–5439. [\[CrossRef\]](#)
59. Antonellis, S.D.; Joppolo, C.M.; Molinaroli, L.; Pasini, A. Simulation and energy efficiency analysis of desiccant wheel systems for drying processes. *Energy* **2012**, *37*, 336–345. [\[CrossRef\]](#)
60. ANSYS. *Fluent Mosaic Technology Automatically Combines Disparate Meshes with Polyhedral Elements for Fast, Accurate Flow Resolution*; ANSYS: Canonsburg, PA, USA, 2018.
61. Sosnowski, M.; Gnatowska, R.; Sobczyk, J.; Wodziak, W. Computational domain discretization for CFD analysis of flow in a granular packed bed. *J. Theor. Appl. Mech.* **2019**, *57*, 833–842. [\[CrossRef\]](#)
62. Sosnowski, M.; Gnatowska, R.; Grabowska, K.; Krzywański, J.; Jamrozik, A. Numerical Analysis of Flow in Building Arrangement: Computational Domain Discretization. *Appl. Sci.* **2019**, *9*, 941. [\[CrossRef\]](#)
63. Eça, L.; Hoekstra, M. A procedure for the estimation of the numerical uncertainty of CFD calculations based on grid refinement studies. *J. Comput. Phys.* **2014**, *262*, 104–130. [\[CrossRef\]](#)
64. Sosnowski, M.; Krzywanski, J.; Scurek, R. A Fuzzy Logic Approach for the Reduction of Mesh-Induced Error in CFD Analysis: A Case Study of an Impinging Jet. *Entropy* **2019**, *21*, 1047. [\[CrossRef\]](#)
65. Celik, I.B.; Ghia, U.; Roache, P.J. Others Procedure for estimation and reporting of uncertainty due to discretization in CFD applications. *J. Fluids Eng. Trans. ASME* **2008**, *130*, 078001.
66. Kakac, S.; Liu, H.; Pramuanjaroenkij, A. *Heat Exchangers: Selection, Rating, and Thermal Design*; CRC Press: Boca Raton, FL, USA, 2012.

